Switching of Cell Proliferation/Differentiation in Thiol-Maleimide Clickable Microcapsules Triggered by *in Situ* Conjugation of Biomimetic Peptides

Yuichiro Oki,[†] Katsuhisa Kirita,[‡] Seiichi Ohta,[§] Shinsuke Ohba,[‡,§] Ikki Horiguchi,[⊥]

Yasuyuki Sakai,[†,‡] and Taichi Ito[*,†,‡,§]

[†]Department of Chemical System Engineering, The University of Tokyo, 7-3-1 Hongo, Bunkyo-ku, Tokyo 113-8656, Japan

[‡]Department of Bioengineering, The University of Tokyo, 7-3-1 Hongo, Bunkyo-ku, Tokyo 113-8656, Japan

[§]Center for Disease Biology and Integrative Medicine, The University of Tokyo, Hongo 7-3-1, Bunkyo-ku, Tokyo 113-0033, Japan

[⊥]Department of Biotechnology, Graduate School of Engineering, Osaka University, 2-1 Yamada-oka, Suita, Osaka 565-0871, Japan

Table of Contents

Table S1: The primer sequences used in reverse transcription quantitative polymerase chain reaction (RT-qPCR) analysis.

Figure S1: Overview of the assumption, geometry, and initial and boundary conditions for the model calculation. By assuming a homogeneous microcapsule distribution, each Alg-Mal microcapsule was assigned to a unit volume of culture medium. This unit volume was chosen as a domain for the model calculation. The model consists of a spherical microcapsule domain using an axisymmetric approximation, which is surrounded by the unit volume of culture media. Orange and red represent the domain of the maleimide-modified alginate microcapsule and its interface with culture media, respectively.

Figure S2: ^{1}H NMR (A) and FT-IR (B) spectra of Alginate (Alg) and maleimide-modified alginate (Alg-Mal).

Figure S3: Observation of Alg-Mal microcapsules via optical microscopy.

Figure S4: Observation of the spatial distribution of the SAMSA-FL by taking the cross-section pictures of the Alg-Mal capsule via confocal laser scanning microscopy. 1 equiv. of SAMSA-FL to maleimide was added to the microcapsule. (B) Time change of fluorescent intensity profile inside the Alg-Mal capsule analyzed by ImageJ. The distance was normalized by the diameter of the microcapsule. (C) Simulated degree of conjugation in Alg-Mal capsule during *in situ* conjugation. Experimental conditions for (A) were used for the calculation. (D) Simulated time change of the conjugation profile of SAMSA-FL inside the Alg-Mal capsule. The distance was normalized by the diameter of the microcapsule. Experimental conditions for (B) were used for the calculation. Scale bar: 200 μm.

Figure S5: Relationship between the degree of conjugation and the SAMSA-FL added to the maleimide moiety after 2 h of immersion (N = 3).

Figure S6: Simulated time change in the degree of maleimide conjugation with SAMSA-FL in Alg-Mal capsules. The initial concentration of SAMSA-FL was 1 equiv. to the maleimide moiety in the microcapsule.

Figure S7: Enlarged view of stained NIH-3T3 cells encapsulated in Alg-Mal microcapsules 7 days after adding RGDS, CRGES, or CRGDS using calcein (green). Results for the sample without peptide addition are also shown as no peptide.

Figure S8: (A) Representative flow cytometry plots using Annexin V-FITC/PI staining for apoptosis. NIH-3T3 cells encapsulated in Alg-Mal microcapsules 1 day after adding RGDS, CRGES, or CRGDS were stained. The positive control (H_2O_2) experiment was performed without addition of any peptide and with addition of H_2O_2. Results for the sample without peptide addition are also shown as no peptide. (B) The percentage of apoptotic cells relative to encapsulated cells. (C) The percentage of necrotic cells relative to encapsulated cells (N=3).

Figure S9: Dependency of cell-proliferation rate on the amount of CRGDS added to the maleimide moiety determined by DAPI assay (N = 3, *: $p < 0.05$).

Figure S10: Cell-proliferation rate after reseeding cells, which was recovered by decomposing Alg-Mal microcapsules with alginate lyase (N = 3).

Figure S11: Effect of *in situ* conjugation of various peptides on collagen production, evaluated by sirius red staining.

Figure S12: (A) Observation of GFP fluorescence in 2D culture of Col1a1GFP-MC3T3E1 cells by confocal microscopy after BMP-2 addition. (B) Effect of BMP-2 addition on cell differentiation evaluated from the fluorescence intensity measured by flow cytometry. GFP fluorescence intensity under each condition was normalized to the control without added peptides (N = 4, **: $p < 0.01$).

Supplementary Note 1
Estimation of characteristic diffusion time and Thiele modulus

Supplementary Note 2
Simulation of reaction-diffusion process in the microcapsule

Table S1. The primer sequences used in reverse transcription quantitative polymerase chain reaction (RT-qPCR) analysis.

GAPDH
F: 5′ AAATGGTGAAGGTCGGTGTG 3′
R: 5′ TGAAGGGGTCGTTGATGG 3′
Col1a1 (Col I)
F: 5′ CTGACTGGAAGAGCGGAGAGTAC 3′
R: 5′ ACAGACGGCTGAGTAGGGAACA 3′
bFGF
F: 5′ GCTATGAAGGAAGATGGACG 3′
R: 5′ GCCACATACCAACTGGAGTATTT 3′
TGF-β
F: 5′ ATCCTGTCCAAACTAAGGCTCG 3′
R: 5′ ACCTCTTTAGCATAGTAGTCCGC 3′

Figure S1. Overview of the assumption, geometry, and initial and boundary conditions for the model calculation. By assuming a homogeneous microcapsule distribution, each Alg-Mal microcapsule was assigned to a unit volume of culture medium. This unit volume was chosen as a domain for the model calculation. The model consists of a spherical microcapsule domain using an axisymmetric approximation, which is surrounded by the unit volume of culture media. Orange and red represent the domain of the maleimide-modified alginate microcapsule and its interface with culture media, respectively.
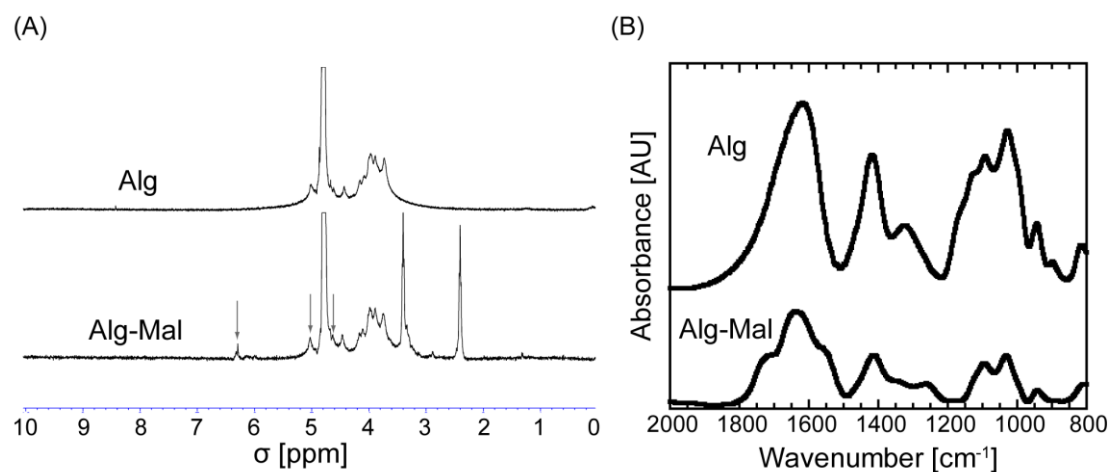
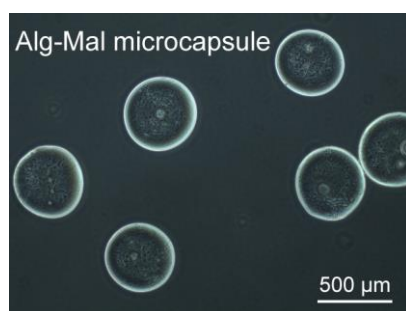**Figure S2.** ^{1}H NMR (A) and FT-IR (B) spectra of Alginate (Alg) and maleimide-modified alginate (Alg-Mal).

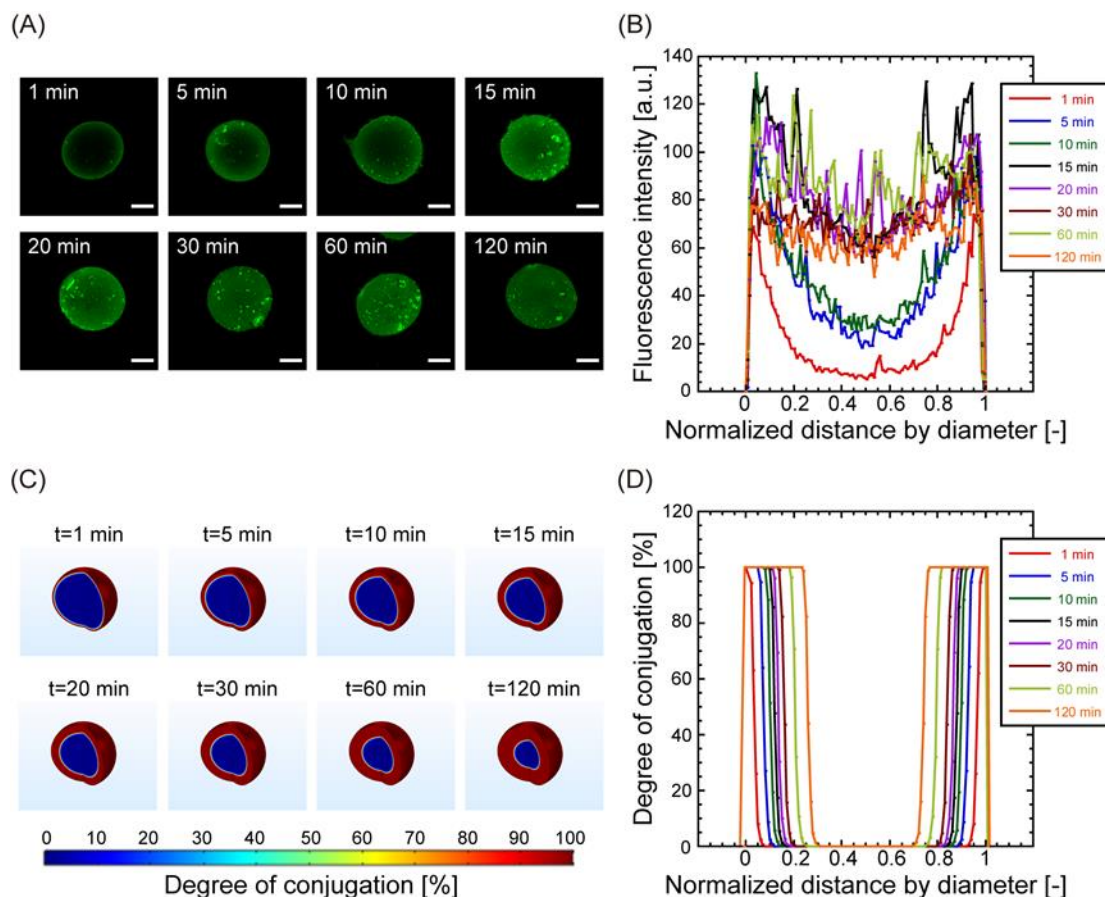**Figure S3.** Observation of Alg-Mal microcapsules via optical microscopy.

Figure S4. (A) Observation of the spatial distribution of the SAMSA-FL by taking the cross-section pictures of the Alg-Mal capsule via confocal laser scanning microscopy. 1 equiv. of SAMSA-FL to maleimide was added to the microcapsule. (B) Time change of fluorescent intensity profile inside the Alg-Mal capsule analyzed by ImageJ. The distance was normalized by the diameter of the microcapsule. (C) Simulated degree of conjugation in Alg-Mal capsule during *in situ* conjugation. Experimental conditions for (A) were used for the calculation. (D) Simulated time change of the conjugation profile of SAMSA-FL inside the Alg-Mal capsule. The distance was normalized by the diameter of the microcapsule. Experimental conditions for (B) were used for the calculation. Scale bar: 200 μm.
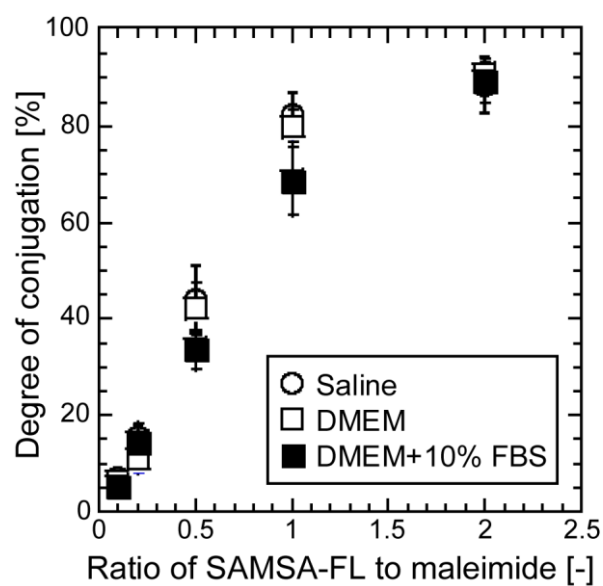
Figure S5. Relationship between the degree of conjugation and the SAMSA-FL added to the maleimide moiety after 2 h of immersion (N = 3).
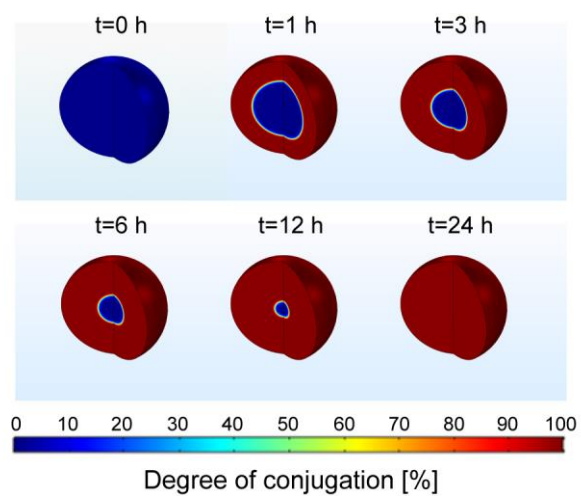

Figure S6. Simulated time change in the degree of maleimide conjugation with SAMSA-FL in Alg-Mal capsules. The initial concentration of SAMSA-FL was 1 equiv. to the maleimide moiety in the microcapsule.
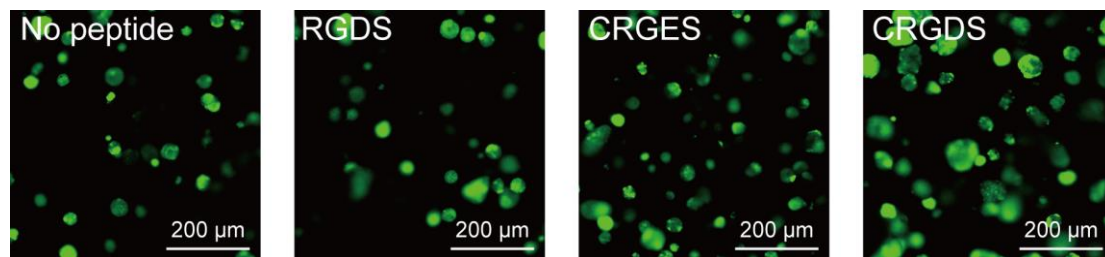
Figure S7. Enlarged view of NIH-3T3 cells encapsulated in Alg-Mal microcapsules 7 days after no addition of any peptide or addition of RGDS, CRGES, or CRGDS. The cells were stained using calcein (green). Results for the sample without peptide addition are also shown as no peptide.
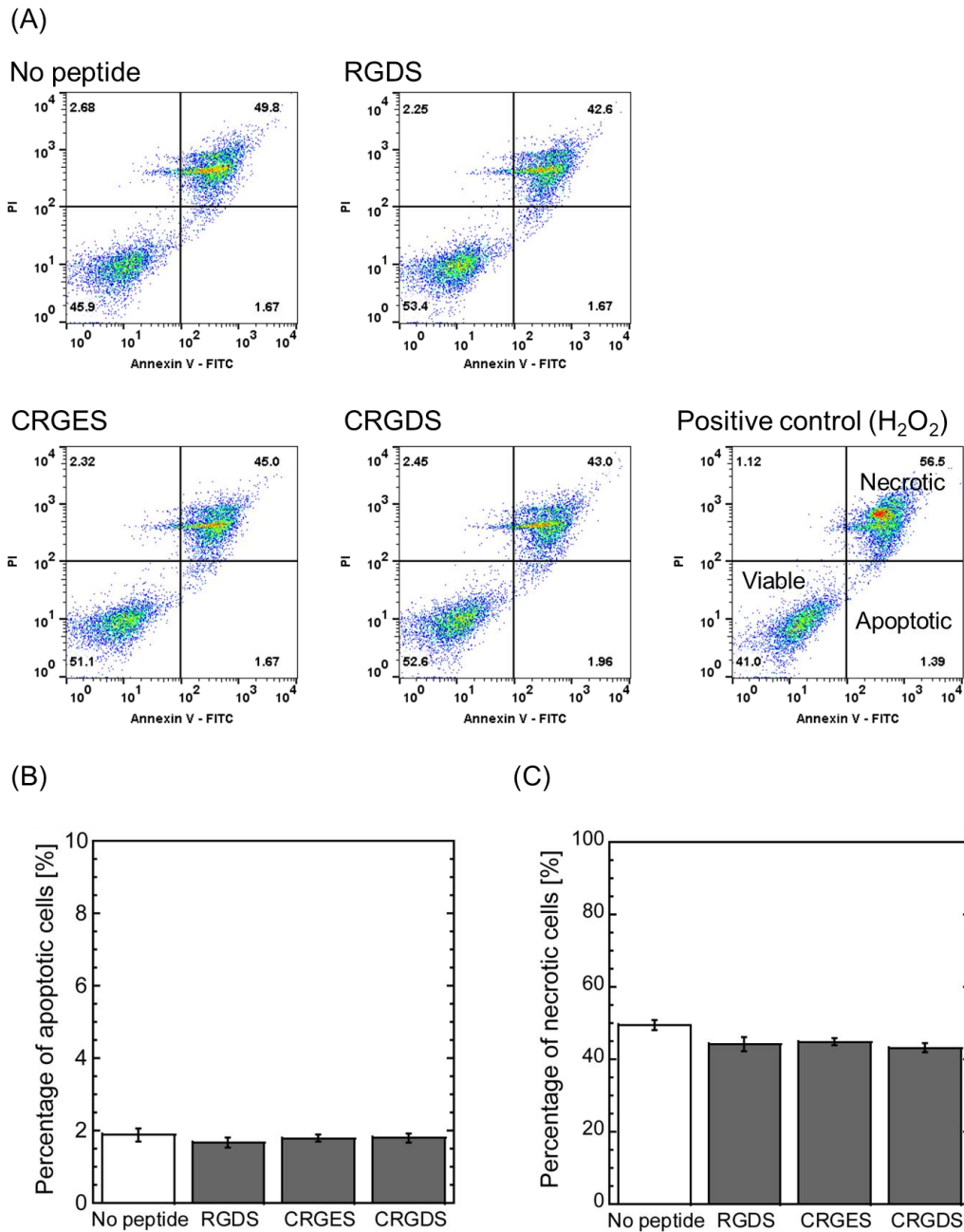
(A)

No peptide

RGDS

CRGES

CRGDS

Positive control (H$_2$O$_2$)

(B)

(C)

Figure S8. (A) Representative flow cytometry plots using Annexin V-FITC/PI staining for apoptosis. NIH-3T3 cells encapsulated in Alg-Mal microcapsules 1 day after adding RGDS, CRGES, or CRGDS were stained. The positive control (H$_2$O$_2$) experiment was performed without addition of any peptide and with addition of H$_2$O$_2$. Results for the sample without peptide addition are also shown as no peptide. (B) The percentage of apoptotic cells relative to encapsulated cells. (C) The percentage of necrotic cells relative to encapsulated cells (N=3).
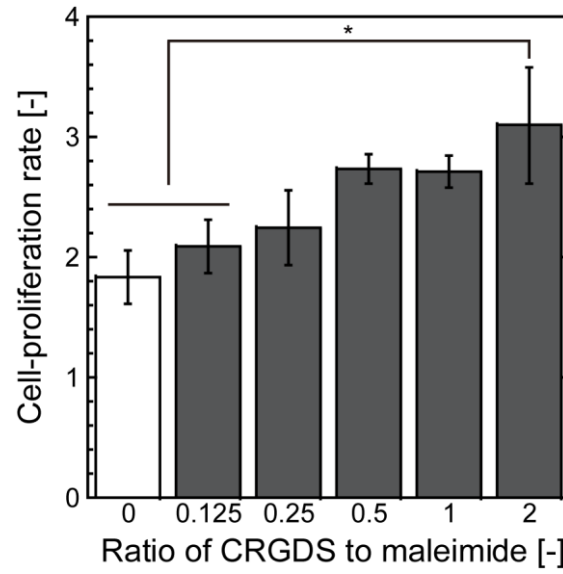
Figure S9. Dependency of cell-proliferation rate on the amount of CRGDS added to the maleimide moiety determined by DAPI assay (N = 3, *: $p < 0.05$).
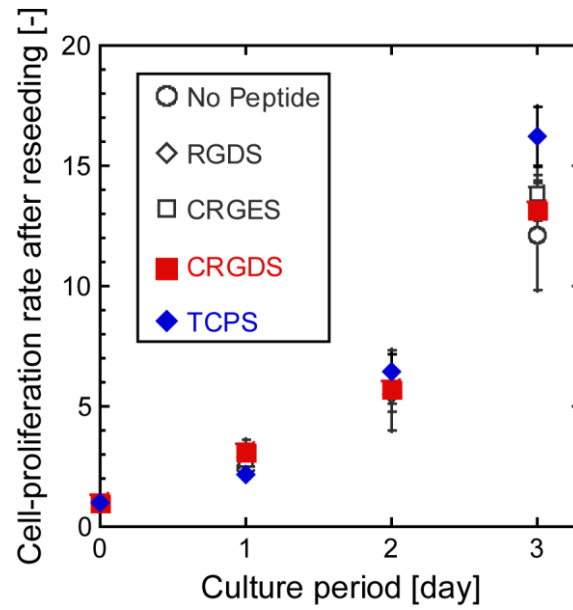

Figure S10. Cell-proliferation rate after reseeding cells, which was recovered by decomposing Alg-Mal microcapsules with alginate lyase (N = 3).
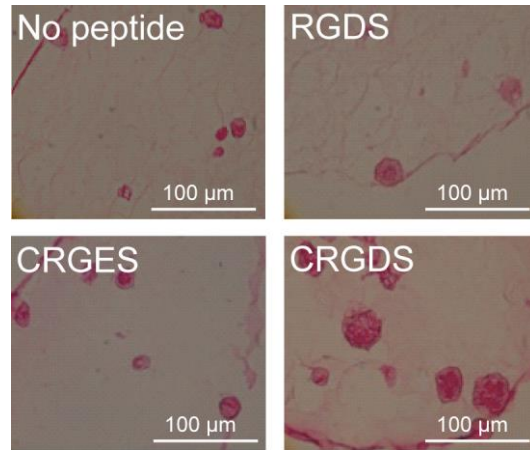
Figure S11. Effect of *in situ* conjugation of various peptides on collagen production, evaluated by sirius red staining.
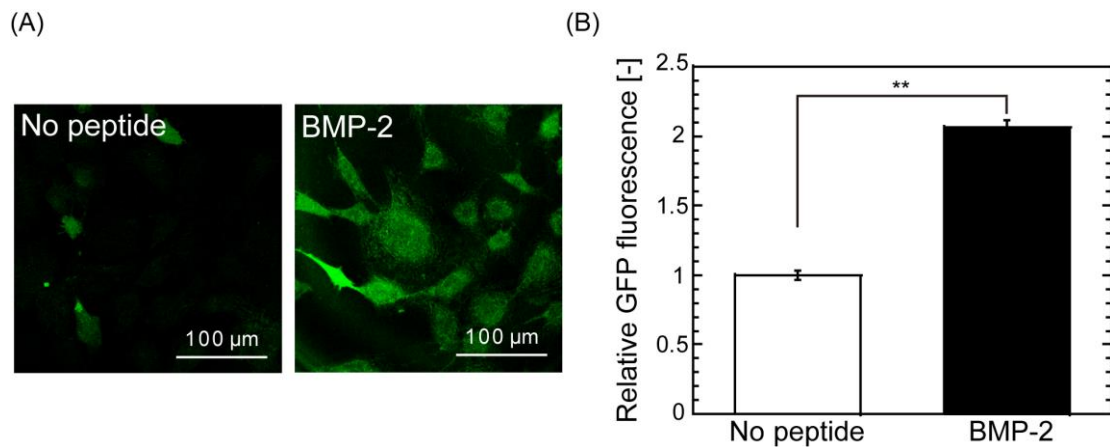

Figure S12. (A) Observation of GFP fluorescence in 2D culture of Col1a1GFP-MC3T3E1 cells by confocal microscopy after BMP-2 addition. (B) Effect of BMP-2 addition on cell differentiation evaluated from the fluorescence intensity measured by flow cytometry. GFP fluorescence intensity under each condition was normalized to the control without added peptides (N = 4, **: p < 0.01).

Supplementary Note 1

Estimation of characteristic diffusion time and Thiele modulus

The characteristic time for the diffusion of SAMSA-FL, τ, was estimated using the following equation based on a previous report [1];

$$\tau = \frac{L^2}{D} \quad (eq.\,1)$$

Here, L and D are the diameter of the microcapsules and diffusion coefficient of SAMSA-FL inside the microcapsule, respectively. Because the hydrodynamic radius of fluorescein, which has a similar chemical structure to SAMSA-FL, is reported as ca. 0.5 nm [2], which is much smaller than the alginate hydrogel matrix, it diffuses rapidly through the Alg matrix due to the negligible resistance of the hydrogel network [3]. Therefore, the diffusion coefficient in the microcapsule, D, is considered almost the same as that in water and can thus be estimated as 4.3×10^{-10} $m^2\,s^{-1}$ using the reported value for fluorescein [2]. Additionally, according to the microscopic observation of microcapsules shown in Figure 2A, the radius of the microcapsules L was ca. 250 μm. By using these values, τ was estimated as 2.4 min, which was consistent with the results in Figure 2A and B.

The Thiele modulus φ was also calculated, according to the following equation based on a previous report [4]:

$$\varphi = L \sqrt{\frac{kC_{int}}{D}} \quad \text{(eq. 2)}$$

Here, k and C_{int} are the reaction rate constant and initial concentration of SAMSA-FL in the media. The reaction rate constant k between DNP-PEG4-Cys and N-(2-aminoethyl)maleimide was reported as $k = 5.2 \times 10^3$ M^{-1} s^{-1} at pH 7.4 [5]. Using this reported value as a representative rate constant, φ was calculated as 5.1 and 27 when C_{int} = 0.035 and 1 mM.

Supplementary Note 2

Simulation of Reaction-diffusion process in the microcapsule

Model Overview, Assumptions and Geometry

The simulation used an axisymmetric domain. Figure S1 shows the model geometry

and boundary and initial conditions of the simulation. By assuming a homogeneous

microcapsule distribution, each Alg-Mal microcapsule was assigned to a unit volume of

culture media. This unit volume was chosen as a domain for the model calculation. It was

assumed that the microcapsule was spherical and that reaction points, i.e., maleimide

groups, were equally distributed in the microcapsule. The diameter of the microcapsule

was assumed to be 500 μm. During reaction-diffusion, the diameter of the microcapsules

and diffusion coefficient of SAMSA-FL were assumed to be constant. Additionally, it was

assumed that SAMSA-FL outside the microcapsule was completely mixed and that there

was no concentration distribution.

Definition of Governing Equations and Parameters

To simulate the *in situ* conjugation of SAMSA-FL and the immobilized maleimide

groups in the microcapsules, the following reaction-diffusion equations were used;

$$\frac{\partial C_{maleimide}}{\partial t} = -k C_{thiol} C_{maleimide} \quad (\text{eq. } 3)$$

$$\frac{\partial C_{thiol}}{\partial t} = \nabla \cdot (D\nabla C_{thiol}) - kC_{thiol}C_{maleimide} \quad (eq.\,4)$$

$$\frac{\partial C_{thiolout}}{\partial t} = -\frac{A}{V} \cdot N_{thiol} \quad (eq.\,5)$$

Here, $C_{maleimide}$ is the concentration of the immobilized maleimide groups. The

concentrations of free SAMSA-FL inside and outside the microcapsule are defined as

C_{thiol} and $C_{thiolout}$, respectively, while k is the rate constant for the reaction between

SAMSA-FL and maleimide groups. The boundary flux of SAMSA-FL was defined as

N_{thiol} at the microcapsule surface. Additionally, A and V are the surface area of the

microcapsules and unit volume of the media assigned to each microcapsule.

For the boundary conditions, the following equation was applied:

$C_{thiol} = C_{thiolout}$ for all the surface of the spherical microcapsule (eq. 6)

$\nabla C_{thiol} = 0$ for the center point of the spherical microcapsule (eq. 7);

$k = 5.2$ m^3 mol^{-1} s^{-1} and $D = 4.3 \times 10^{-10}$ m^2 s^{-1} were used for the calculation, according

to previous reports [2, 5]. $A = 7.9 \times 10^{-7}$ m^2, $V = 1.0 \times 10^{-8}$ m^3, $C_{maleimide,initial} = 5.3$ mol

m^{-3}, $C_{thiol,initial} = 0$ mol m^{-3}, and $C_{thiolout,initial} = 3.5 \times 10^{-2}$ or 1.0 mol m^{-3} were used based

on the experiments.

Numerical Implementation

The equations were solved using a commercial finite element package, COMSOL

Multiphysics version 5.4 (COMSOL Multiphysics Burlington, MA). The COMSOL

module, *Transport of Diluted Species*, was used to solve equations 3–7. The mesh comprised triangular elements with minimum and maximum sizes of 0.01 and 5 μm, respectively. The relative tolerance was set as 0.005. A backward differentiation formula stepping algorithm was used with a maximum time step of 1 s thereafter. It was confirmed that even if the mesh size and time step were smaller, the calculation result would hardly be affected.

Supplementary References

(1) Chaparro, M. C.; Saaltink, M. W.; Soler, J. M.; Slooten, L. J.; Mader, U. K., Modelling of Matrix Diffusion in a Tracer Test in Concrete. *Transp. Porous Med.* **2016**, *111*, 27–40

(2) Schuster, E.; Sott, K.; Strom, A.; Altskar, A.; Smisdom, N.; Geback, T.; Loren, N.; Hermansson, A., Interplay between flow and diffusion in capillary alginate hydrogels. *Soft Matter.* **2016**, *12*, 3897-3907.

(3) Amsden, B., Solute Diffusion within Hydrogels. Mechanisms and Models. *Macromolecules* **1998**, *31*, 8382–8395.

(4) Magyari, E., Exact analytical solutions of diffusion reaction in spherical porous catalyst. *Chem. Eng. J.* **2010**, *158*, 266–270.

(5) Fontaine, S. D.; Reid, R.; Robinson, L.; Ashley, G. W.; Santi, D. V., Long-Term

Stabilization of Maleimide–Thiol Conjugates. *Bioconjug. Chem.* **2015**, *26*, 145–152.